Science of the Total Environment 838 (2022) 156064

Contents lists available at ScienceDirect

Science of the Total Environment

journal homepage: www.elsevier.com/locate/scitotenv

Detection and assessment of marine litter in an uninhabited island, Arabian Gulf: A case study with conventional and machine learning approaches

S. Veerasingam, Mark Chatting, Fahad Syed Asim, Jassim Al-Khayat, P. Vethamony *

UNESCO Chair in Marine Sciences, Environmental Science Center, Qatar University, P.O. Box: 2713, Doha, Qatar

HIGHLIGHTS

- Machine learning method was used to automatically detect marine litter.
- Models were trained with over 10,400 images extracted from field videos.
- The best model had 91% of mAP and well match with field data.
- Machine learning is a rapid tool for the long-term marine litter monitoring programs.

GRAPHICAL ABSTRACT

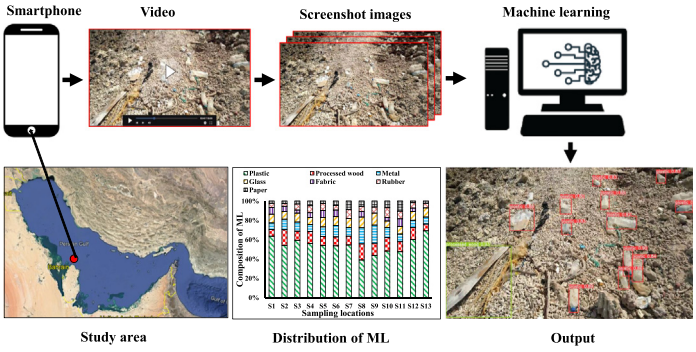

ARTICLE INFO

Editor: Damià Barceló

Keywords:
Marine litter
Plastics
Machine learning
YOLO-v5
Ras Rakan Island of Qatar

ABSTRACT

In 2018, the Ministry of Municipality and Environment, Qatar removed 90 t of marine litter (ML) from the Ras Rakan Island (RRI), a remote uninhabited island in the Arabian Gulf (hereinafter referred to as Gulf). To identify the sources of ML and understand the post-cleaning ML accumulation rate, a ML survey was conducted around RRI in 2019. A total of 1341 ML items were found around RRI with an average abundance of 3.4 items/m^2. In addition, a machine learning approach was applied to extract the quantity and types of ML from 10,400 images from the sampling sites (beaches) to make the ML clean-up process and monitoring effort more efficient. The image coordinates of ML objects were used to train an object detection algorithm 'You Only Look Once (YOLO-v5)' to automatically detect ML from video data. An image enhancement technique was performed to improve the quality of unclear images. The best performing YOLO-v5 model had 90% of mean Average Precision (mAP) while maintaining near real-time processing speeds at 2 ms/image. The abundance of ML around RRI was higher than that found on the coast of mainland Qatar. 61.5% of the sampling locations are considered as 'extremely dirty' based on Clean Coast Index. Windward beaches had higher ML concentrations (derived from neighbouring countries) than the leeward beaches. Like RRI, most of the uninhabited islands in the Arabian Gulf are home to many seabirds and sea turtles, and could act as major sinks for ML deposition. Therefore, implementation of this machine learning technique to all islands allows estimating and mitigating the load of ML for achieving a sustaining and a cleaner ocean.

* Corresponding author.
E-mail addresses: v.subramanian@qu.edu.qa (S. Veerasingam), mchatting@qu.edu.qa (M. Chatting), fahad.syed@qu.edu.qa (F.S. Asim), jalkhayat@qu.edu.qa (J. Al-Khayat), pvethamony@qu.edu.qa (P. Vethamony).

http://dx.doi.org/10.1016/j.scitotenv.2022.156064
Received 22 March 2022; Received in revised form 28 April 2022; Accepted 16 May 2022
Available online 18 May 2022

1. Introduction

Accumulation of marine litter (ML), especially plastic debris in different environmental compartments (beaches, islands, surface and sub-surface water and food web) situated between north and south poles has been increased in the past few decades (Monteiro et al., 2018). Though ML consists of plastic, glass/ceramic, metal, wood, paper, textile and rubber (EC JRC, 2013), plastics are the most dominant (60–80%) litter in the marine environment (Barboza et al., 2019). These anthropogenic ML causes the most relevant risks on human health as well as environmental and ecological health consequences (Filho et al., 2019). The negative impacts of ML in the marine environment include entanglement (Gregory, 2009; Thiel et al., 2018), ingestion (Savoca et al., 2021), bioaccumulation of persistent organic and inorganic pollutants (Teuten et al., 2009; Ranjani et al., 2022), and transfer of non-native species through hitchhiking (Al-Khayat et al., 2021). In addition to negative consequences on marine biodiversity, ML also negatively affects the economy of many coastal countries (McIlgorm et al., 2011; Beaumont et al., 2019). Nearly 80% of anthropogenic ML enters the sea from land-originated sources, whereas 20% is derived from sea-based sources (EC JRC, 2013). Borrelle et al. (2020) estimated that ~19 to 23 MT of plastic wastes were generated in 2016 globally, and finally entered in the aquatic ecosystems.

Once ML enters in the ocean, it can travel to long distances (even to remote islands) by ocean currents and winds (Maximenko et al., 2012; Iwasaki et al., 2017). According to Burt et al. (2020), globally, small islands receive unprecedented amount of anthropogenic ML. In the Arabian Gulf, due to environmental, geological and climatic diversity some of the islands are inhabited (e.g., Qeshm Island), whereas most of the islands are uninhabited. Since the countries bordering ROPME (Regional Organization for the Protection of the Marine Environment) Sea Area are undergoing rapid economic and population growth, land-based ML is also growing fast in the past few decades (Al-Salem et al., 2020; Lyons et al., 2020; Uddin et al., 2020; Veerasingam et al., 2020a). Moreover, the Gulf being the leading oil producer in the world, the discharge of ML through shipping, fishing and industrial activities are also increasing (Kor and Mehdinia, 2020). Though the distribution of ML has been reported for the mainland of Gulf (Sarafraz et al., 2016; Veerasingam et al., 2020a), the ML accumulation trend on the isolated islands is relatively very scarce.

Traditional analysis of ML video data that requires watching videos in real time is time consuming and remains as a significant obstacle in achieving regional scale ML assessments (Martin et al., 2021). Though, various ML monitoring methods have been developed and applied, they are not comparable in many cases. Therefore, standardized automated ML detection methods are required to solve this problem. For this reason, several field ML videos and images and different image processing methods need to be applied (Hidaka et al., 2022). The exponential growth in computational speed and artificial intelligence techniques have attracted the environmental scientists and provided new opportunities in efficient pollution monitoring. Machine learning is a data-driven approach that trains a regression or classification model through a complex nonlinear mapping with adjustable parameters based on a training dataset (Yu and Ma, 2021). Very recently, this sort of rapid, cost-effective and easily reproducible machine learning techniques has increased in assessing the ML (Kylili et al., 2019, 2021; Garcia-Garin et al., 2021; Politikos et al., 2021; Lin et al., 2021; Marin et al., 2021; Gomez et al., 2022). As Machine Learning approaches are getting more sophisticated, neural networks are able to learn specific features of pre-determined classification classes of a wide array of input data (for example: audio, image, text and other data) (Wu et al., 2021). Subsequently, machine-learning models can perform data analysis of complex video/image data several orders of magnitude faster than human, and if trained to a sufficient level of accuracy, perform these tasks more accurately than human (Ditria et al., 2020).

In recent years, the YOLO (You Only Look Once) algorithm series have provided fascinating outputs in different sub-areas of object detection. One of the notable features of this method is the fast detection speed. We find that this technique is not used in any of the studies related to ML in the Arabian Gulf. Therefore, in this study, we have applied YOLO algorithm using conventional neural networks to prove its efficiency in the beach litter object detection. Ras Rakan Island (RRI) is one of the uninhabited islands in the Arabian Gulf, which also acts as a home for breeding of sea birds (especially, *Phalacrocorax nigrogularis*) and sea turtles (especially, *Eretmochelys imbricata*) (Kardousha et al., 2016; Muzaffar, 2020; Mark et al., 2021) (Fig. S1). The Ministry of Municipality and Environment (MME), State of Qatar has carried out a cleaning campaign in RRI during April 2018, and 90 t of ML (Fig. S2) were removed (MME, 2018). Following this in October 2019 (i.e., after one year of this major cleaning campaign), we have conducted a ML survey with the following objectives: (i) to understand the current ML distribution pattern around the RRI, (ii) to characterize the composition of ML and identify their sources, and (iii) to test the efficiency of the machine learning technique, YOLO-v5 in detecting the beach ML using high-resolution video images.

2. Materials and methods

2.1. Study area

The Gulf coastline is ~3700 km in length with several cities on the Arabian side than the Iranian shore. Thus, substantial and gradually growing stress is exerted on the marine resources of the region with associated large-scale degradation of coastal ecosystems (Al-Cibahy et al., 2012). The Exclusive Economic Zone (EEZ) of Qatar consists of nearly 31 natural islands, most of them located on the northern and eastern sides of the peninsula. RRI is an uninhabited island located nearly 2 km north of the mainland (Arekhi et al., 2020). It is 'T' shaped island with a length of 3.5 km in the east-west orientation (Fig. 1). In most part of the island, the width is 100 m, except at the western side, where the width is around 400 m (Veerasingam et al., 2021). This island is vegetated with shrubs, plants, sabkha and bushes. It is made up of limestone carbonate rocks of Dammam Formation of Middle Eocene age. The southern part of the Island is clayey, where mangroves with Sabkha are present (Rajendran et al., 2021). RRI is home for sea turtles and sea birds breeding. Socotra Cormorant birds (*Phalacrocoras nigrogularis*) are regionally endemic, locally abundant species, primarily restricted to the Gulf. This species is currently categorized as vulnerable by the International Union for Conservation of Nature (Muzaffar et al., 2017).

2.2. ML sampling and identification of rafting species

The team from Environmental Science Center, Qatar University conducted ML survey at 13 locations around RRI in October 2019 (Fig. 1). At each location, a section/transect covering an area of 250 m^2 (50 m length and 5 m wide) was sampled. Video recording of the beaches was performed with a smartphone, having a resolution of 1920 × 1080 and at 24fps. ML items, larger than 2.5 cm presented within the transects were considered for this study. ML items were classified as plastic, glass, metal, fabric, paper, processed wood and rubber (OSPAR, 2010). The hitchhiking organisms associated with ML were identified under a dissecting microscope to the lowest possible level using the available identification keys and literature (Jones, 1986; Oliver, 1992; Bosch et al., 1995; Richmond, 2002; Shahdadi et al., 2014; Shabani et al., 2019; Al-Khayat et al., 2021).

2.3. Clean Coast Index

The Clean Coast Index (CCI) is a tool to assess the level of cleanliness of the beach (Alkalay et al., 2007). To evaluate the state of, being free from ML or not, each sampling location, CCI was calculated using the formula: $CCI = C_{ML} \times K$, where K is a constant ($K = 20$) and C_{ML} is the density of ML items per m^2. The beaches were classified as 'clean' to 'extremely dirty', based on the scale provided and the amount of ML found on each beach. The CCI values are categorized as very clean (0 to 2), clean (2 to 5), moderately clean (5 to 10), dirty (10 to 20), and extremely dirty (>20). Thus, CCI assessment method gives a cumulative indicator, which explains the quality

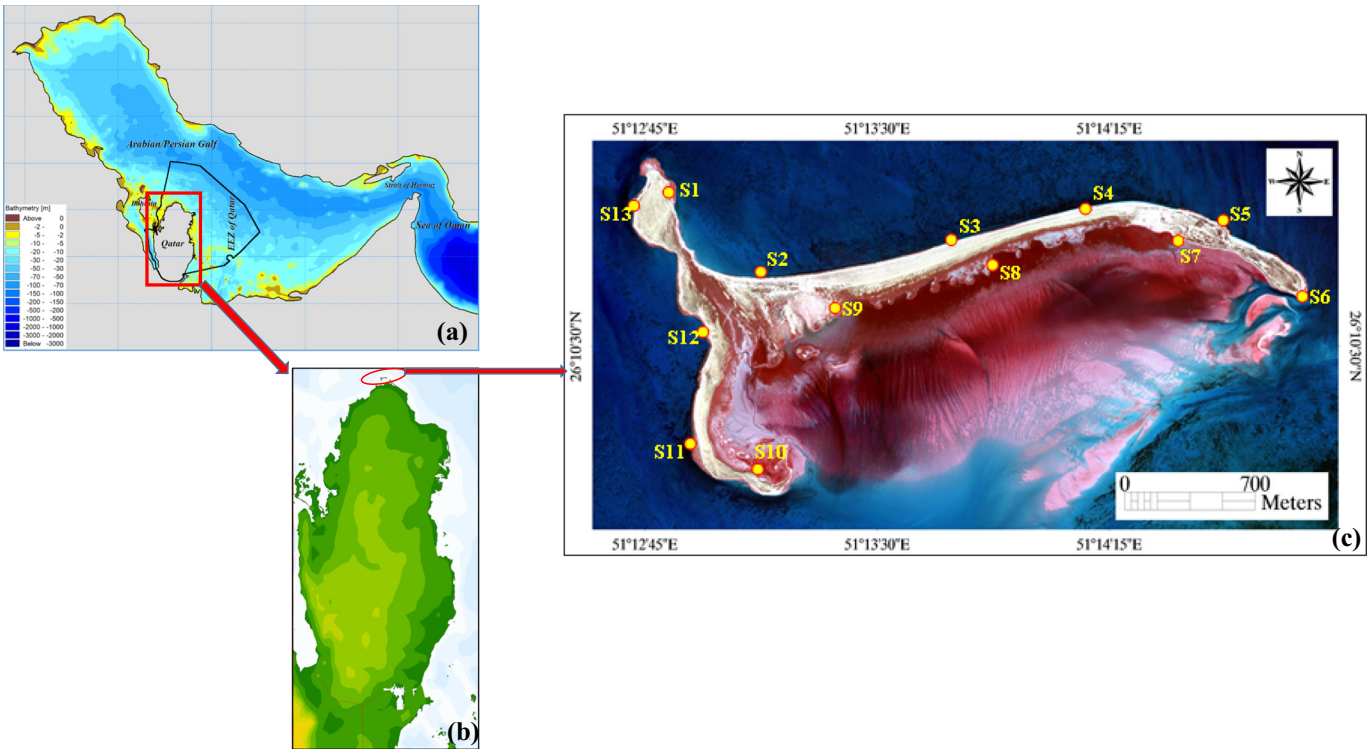

Fig. 1. (a) The bathymetry map of the Arabian Gulf and EEZ of Qatar, (b) location of Ras Rakan Island, and (c) The study area and ML sampling locations along the beaches of Ras Rakan Island.

of beaches in terms of potential and direct damage to the health of marine organisms (Veerasingam et al., 2020b).

2.4. Hazardous Litter Index

The Hazardous Litter Index (HLI) is used to assess the possibility of being affected by hazardous items (that can pierce or cut) such as metal and glass and toxic waste in beach (Rangel-Buitrago et al., 2019a). The HLI value of each location was calculated using the formula:

$$HLI = \frac{\sum HazardousML}{\log_{10}\sum TotalML} \times K$$

HLI allows evaluating the environmental quality of beach in terms of hazardous items in five classes that range from I to V (Table S1).

2.5. Machine learning

2.5.1. YOLO-v5 algorithm

YOLO is an algorithm that utilizes a single conventional network for object detection. YOLO algorithm has undergone six generations (YOLO-v1 to YOLO-v6) of changes and evolutions. The fifth generation of YOLO (YOLO-v5) has great advantage in speed and accuracy compared to its four previous generations. YOLO-v5 exhibits optimal performance on Microsoft COCO (common objects in context). YOLO-v5 consists of four parts such as (i) Input, (ii) Backbone: Cross Stage Partial Network (CSPDarknet), (iii) Neck (PANet), and (iv) Head (YOLO layer) (Xu et al., 2021). Based on the depth of network and the width of feature map, YOLO-v5 is divided into four models such as YOLO-v5s, YOLO-v5m, YOLO-v5l, and YOLO-v5x. These four models represent the trade-offs between increasing accuracy, decreasing classification speed and increased computational resources for training. In this study, considering the speed and accuracy, YOLO-v5m was selected as the model for ML detection and classification.

The YOLO-v5 algorithm partitions the input image into S × S grids with every grid cell being accountable for the recognition of an object if the center of that body falls into that grid cell. Predefined anchor boxes are created in each grid of the input image and generate bounding boxes. Five predictions such as x, y, w, h, and confidence score are contained in each bounding box. The coordinates x and y represent the center of the predicted bounding box relative to the boundaries of the grid. The width and height of the predicted bounding box relative to the entire image are w and h, respectively (Redmon et al., 2016; Kylili et al., 2021). The intersection over union (IoU) between the predicted and the ground truth bounding box is considered as the confidence score. Bounding boxes, having confidence scores higher than the threshold of 0.5, were considered for identification of ML items in the image or video. Moreover, a set of C class probabilities is predicted for each grid cell containing a ML item. Then, the confidence score is multiplied by the class probability of each bounding box to produce its class-specific confidence score. The box containing the highest class-specific confidence score is selected for the final prediction.

2.5.2. Training the model

The flowchart of model training is given in Fig. 2. The dataset was curated by collecting videos of ML along the beaches of RRI. Images were taken from 13 videos which recorded at 12 frames per second (fps). These images of ML items were labeled and categorized as plastic, glass, metal, paper, fabric, rubber and processed wood. The technical description of the proposed dataset is given in Fig. S3. After labelling, data augmentation was used to extend the dataset size and enrich the data for the model to be trained on. Data augmentation techniques including rotation, scaling, shearing and translation were used in this model to increase the amount of data available for model training. A training-testing data split was performed, where 80% of the images were randomly chosen for model training, and the remaining 20% were assigned to test the model. The corresponding ground truth mask of ML item was manually drawn using the 'label_img' annotation tool for training and testing set images. In order to evaluate the model, the ground truth bounding boxes are important. By comparing each of them with the predicted boxes, it is possible to calculate

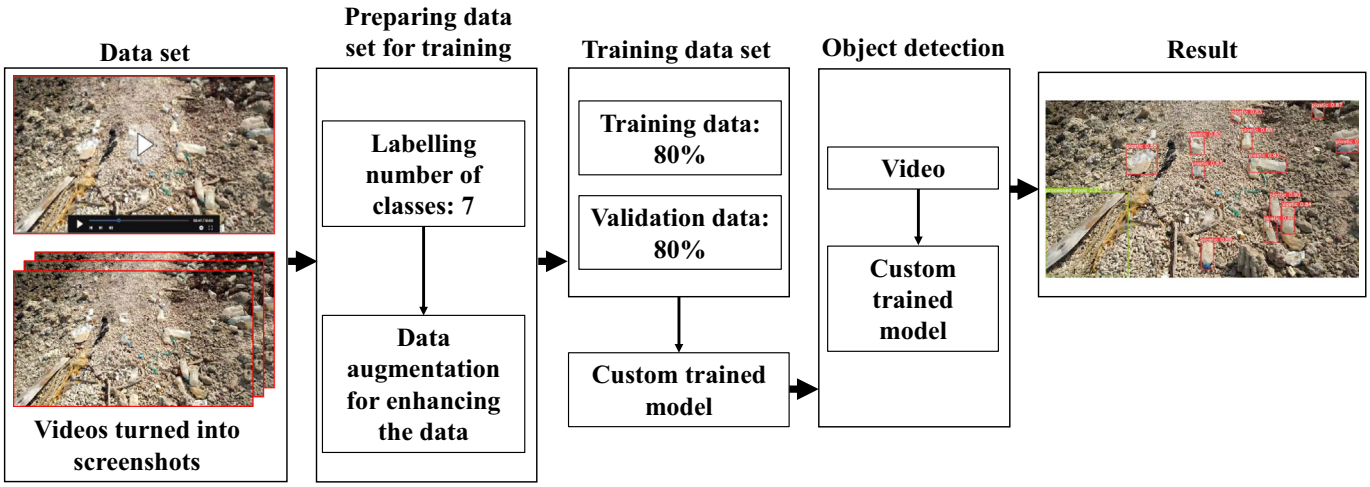

Fig. 2. The framework of the ML detection network. The flow chart is showing the various steps involved in the ML detection model training based on YOLO-v5 algorithm.

the loss of the training, average precision and the validation processes. Drawing on the size of ML items in the training and the validating images, the machine learning method is subsequently charged with the task of recognizing, localizing and segmenting the ML.

2.5.3. Evaluation matrices

The labeled ML items were dubbed as ground truth objects. The YOLO-v5 algorithms detected ML items from each image during the training and validation processes. The intersection over union (IoU) was calculated using the following formula to compare the findings with the ground truth ML items.

$$IoU = \frac{|A \cap B|}{|A \cup B|}$$

where, A and B are the bounding boxes of predicted and the ground truth images, respectively. The predicted bounding box is a rectangular box assigned by trained model during detection on each identified ML item. The ML items with IoU values <0.5 were not considered in this study since they indicate a low level of confidence. For each ML class, based on the area under the precision and recall curve, accuracy of the YOLO-v5 method was retrieved. The aggregate average precision (AP) of the model is derived from the average of all accuracy values. The following equations were used to calculate the precision and recall for each ML class:

$$Precision = \frac{TP}{TP + FP}$$

$$Recall = \frac{TP}{TP + FN}$$

where, TP denotes true positives (i.e., the total number of ML items correctly labeled by the model belongs to the correct class). FP refers to the false positives (i.e., the total number of ML items incorrectly labeled by the tool to fall under the correct class).

Based on the precision (P) and recall (R) rates, the mean average precision (mAP) is determined. The curve with R as the horizontal axis and P as the vertical axis is referred to as the PR curve. The AP value is calculated, based on the area under PR curve, using the following formula:

$$AP = \int_0^1 PdR$$

The average of the average accuracy of all ML items is the mAP value, as shown below:

$$mAP = \frac{\sum_{i=1}^{N} AP_i}{N}$$

where, N denotes the total number of detected ML categories.

3. Results and discussion

3.1. Spatial distribution and composition of ML

During the ML survey in the RRI in October 2019, a total of 1341 items were found. ML densities ranged between 1.1 and 5.5 items/m^2 with an average of 3.4 items/m^2. The spatial distribution of ML exhibited higher densities in the western and northern parts of the Island, whereas lower densities were observed in the southern part of the Island, i.e., windward beaches had higher ML concentrations than the leeward beaches (Fig. 3). The average density of ML observed in the RRI was higher than those found in the mainland of Qatar (1.98 items/m^2; Veerasingam et al., 2020b). Moreover, the average ML density of RRI was found to be higher compared to other islands around the world (for example, Trindade Island, Brazil (2.5 items/m^2; Andrades et al., 2018), Isla Arena Island, Colombia (2.87 items/m^2; Rangel-Buitrago et al., 2019b), Mukkawar Island, Red Sea (0.23 items/m^2; Ibrahim et al., 2020), Lord Howe Island, Australia (2.18 items/m^2; Grant et al., 2021)). However, lower than those found in some of the global islands such as Henderson Island, South Pacific (239.4 items/m^2; Lavers and Bond, 2017) and Keeling Islands, Australia (3.6 items/m^2; Lavers et al., 2019).

The composition of ML around the RRI showed that plastic items were the most abundant (54.01%), followed by processed wood (11.24%), metal (10.22%), glass (9.16%), rubber (6.32%), fabric (4.24%), and paper (4.81%). At all sampling locations, though plastic items were the abundant material, there were differences in the abundance of other items. The average composition of ML around the RRI was lesser than the global average (Galgani et al., 2013). In spite of major ML cleaning activities carried out in 2018, and subsequently 90 t of wastes were collected, still huge amount of ML has been accumulated around the Island within one year (Fig. S4).

3.2. Sources of ML

The ML items found around the RRI were contributed by the following sources: (i) land-based, (ii) sea-originated, and (iii) unknown sources. Overall, 71% of ML falls under 'land-based', followed by 19% sea-based and 10%

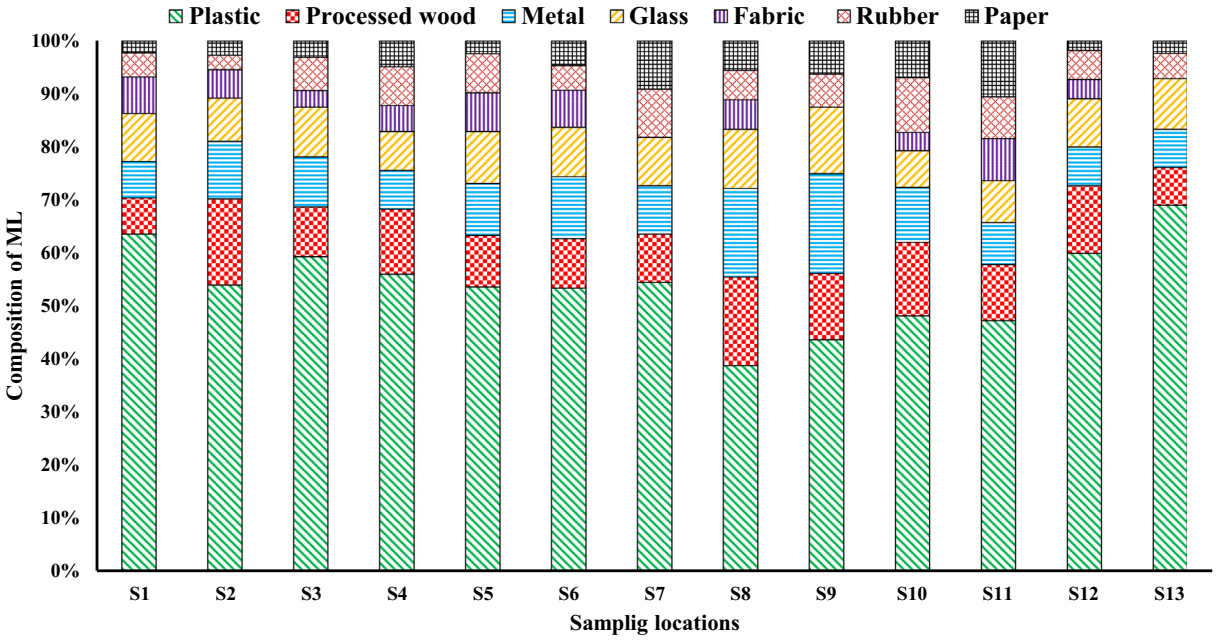

Fig. 3. Abundance, spatial distribution and composition of ML in thirteen locations around the Ras Rakan Island.

unknown sources. The country of origin of ML (especially PET bottles) was determined based on the manufactured place, language and barcode (Veerasingam et al., 2020b). It is interesting to observe that most of the ML items found on the windward side of RRI were transboundary nature (i.e., derived from neighbouring countries - Bahrain, Saudi Arabia, Iraq and UAE), whereas ML items found on the leeward side were from Qatar (Fig. S5). Earlier studies indicated that the transports of ML items in the Gulf are controlled by three factors: winds, currents, and Stokes drift (Veerasingam et al., 2020a, 2020b; Al-Khayat et al., 2021). The winds and Stokes drift are predominantly from the NW/NNW direction, while the currents are in the SE direction. These forces carry the ML from the northern Gulf to the west coast of Qatar, and part of it settles along the beaches. Recently, Veerasingam et al. (2021) identified considerable amount of microplastics on the beach sediments of the RRI. The overall inference is that the net wind and hydrodynamic forcing enables a shoreward transport of ML on the west of RRI, which ultimately causes the settlement of ML along the western beaches in definite proportion. ML survey informs that RRI is receiving a huge quantity of trans-boundary items from the neighbouring countries, and clearly indicates that RRI acts as a sink for plastic debris derived from both land and sea-based sources (Veerasingam et al., 2020b).

3.3. Assessment of beach quality

The quality of beach was evaluated based on the accumulation of ML and various beach quality assessment indices (Mugilarasan et al., 2021). Based on the clean coast index (CCI), we categorized 61.54% of the studied locations as 'extremely dirty', 23.08% sites as 'dirty' and 15.38% as 'moderately clean' (Fig. 4). Most of the sampling locations on the windward beaches fall under 'extremely dirty', while the leeward beaches are mostly 'moderately clean to dirty' category. Hazardous ML items can have public

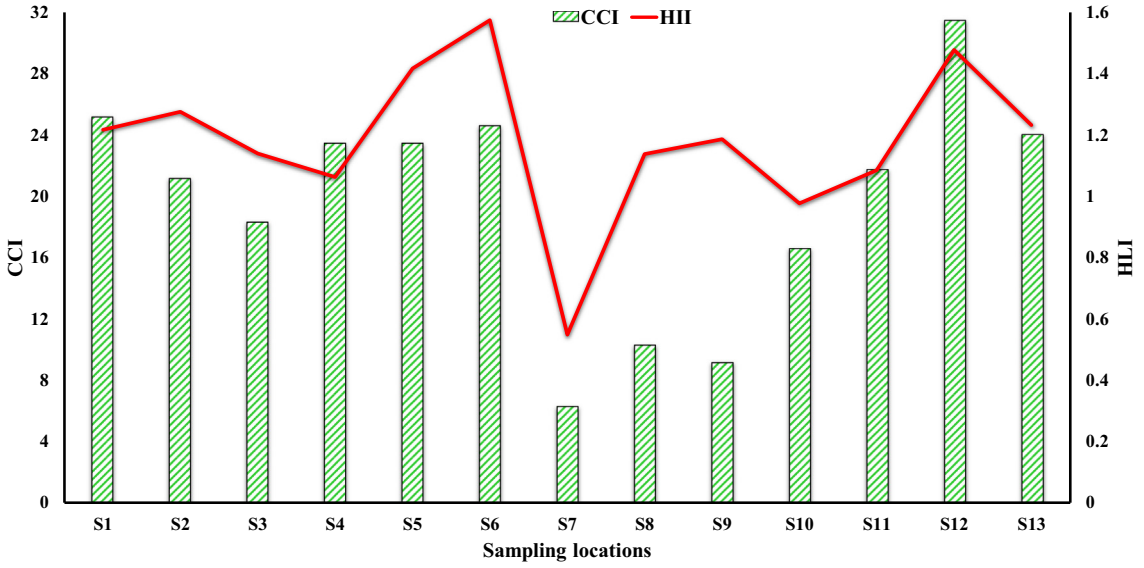

Fig. 4. Assessment of quality of beaches around the Ras Rakan Island are categorized based on the Clean coast index (CCI) and Hazardous Litter Index (HLI) values.

health implications, for example, sharp edged broken glass items and metal cans can cause injuries (Mugilarasan et al., 2021). Moreover, toxic items such as sanitary waste and medical waste (syringe needles) can cause direct and indirect physiological damages (Rangel-Buitrago et al., 2019a). The calculated average Hazardous Litter Index (HLI) values of windward beaches on the RRI were higher (1.3) than those found on the leeward beaches (0.96). Overall, the beaches were categorized based on HLI values from Class II to III (Table S1), i.e., 'little to no hazardous ML observed' to 'a considerable amount of hazardous ML observed' (Fig. 4). Since RRI is an uninhabited island and used very little by boaters or public, it is prudent to assume that most of the ML found along the beaches were derived from sources that are located outside the island.

3.4. Rafting species composition

Though most of the ML items were clean and freshly looking items (manufactured year between 2018 and 2019), 10% of items were degraded and associated with encrusting organisms (Fig. S6). The most common fouling phyla found on the items were Anthropoda, Mollusca and Bryozoa. Overall, *Amphibalanus amphitrite* is the abundant rafting species found around the RRI. Recently, Al-Khayat et al. (2021) found that beaches along the west coast of Qatar receive a huge quantity of bio-fouled floating materials, which cause great damage to biodiversity. The present study also confirms that the trans-boundary items could be a potential vector for the introduction of non-indigenous species to the EEZ of Qatar.

3.5. Training, testing, validating and estimating the prevalence of ML

A total of 10,400 photos containing 41,878 annotations of ML items were used (Fig. 5) in this study. Despite the intrinsic characteristics of the dataset, the performance of YOLO-v5 was better aligned with other ML monitoring studies (Martin et al., 2018; Fallati et al., 2019; Goncalves et al., 2020). Instances of classes used for model training followed a comparable composition of field observations (Fig. 5). Plastic (59.02%) was the greatest proportion of ML annotations used in model training, followed by processed wood (25.40%), fabric (5.92%), glass (3.54%), metal (2.96%), rubber (1.65%) and paper (1.57%). The representative evaluation indicators of the improved model are shown in Fig. 6. Training was terminated at 150 epochs as it was clear that validation loss and accuracy curves had stabilized (Fig. 6a and b). The neural network succeeded in predicting different categories of ML items, and obtained an overall mean average precision (mAP) of 0.91 (Fig. 6a). Moreover, the trained network mAP values for plastic, glass, metal, paper, fabric, rubber and processed wood were 0.92, 0.96, 0.97, 0.96, 0.88, 0.84, and 0.83, respectively. The accuracy levels of mAP values obtained in this study were higher than those found in other studies that have employed object detection algorithms. For example, the YOLO algorithm applied to identify the sea cucumbers and fish had accuracy levels of only 76% and 54%, respectively (Xia et al., 2018; Xu and Matzner, 2018). Ditria et al. (2020) obtained higher accuracy of mAP (> 92%) with YOLO algorithm when detecting a single species of fish from video data. Large variations in accuracy among the object detection models could be attributed to varying amounts of training data. For example, Xia et al. (2018) have achieved 76% accuracy using a total of 150 annotations to train their model, which is considerably lower than that was used in the present study. Wang et al. (2019) have applied the data augmentation techniques (similar to the technique used in the present study) and found better accuracy in object detection models, though they have used a small dataset.

We have found a significant positive correlation between the ML data obtained using conventional method and machine learning method, especially for the plastic litter distribution ($r^2 = 0.9$). Therefore, these results showed that the machine learning algorithms can be effectively used to automate ML detection (especially, plastic litter detection) and classification from video and imagery data with a relatively high degree of accuracy. The time consuming and expensive manual classification of ML items from video data can be eliminated using this approach, which would enable analysis of large size video datasets. Errors in detection of ML could be attributed to false detections of background image features and complexity of dataset. However, previous research showed that an object detection model trained to identify a single fish species has achieved better accuracy (i.e., mAP >92%) than the human effort (Ditria et al., 2020).

3.6. Future management considerations for the integrated ML monitoring for the islands

The Gulf has many islands, mostly small, distributed in the entire Gulf. Within the EEZ of Qatar itself, there are nearly 31 islands, enriched with variety of marine ecosystem. These islands are home for breeding of seaturtles and seabirds. The present study identified RRI as a sink to ML, and more or less similar scenarios can be expected in other islands of Qatar as well as in the Gulf. Moreover, ML on the beaches creates physical barriers,

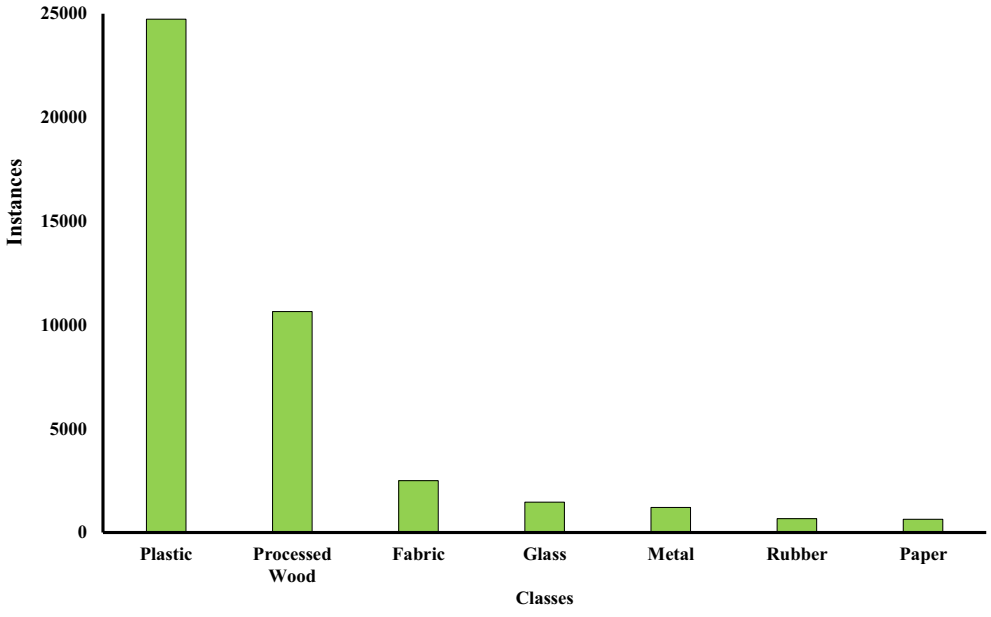

Fig. 5. Total number of annotations of marine litter items assembled in each class.

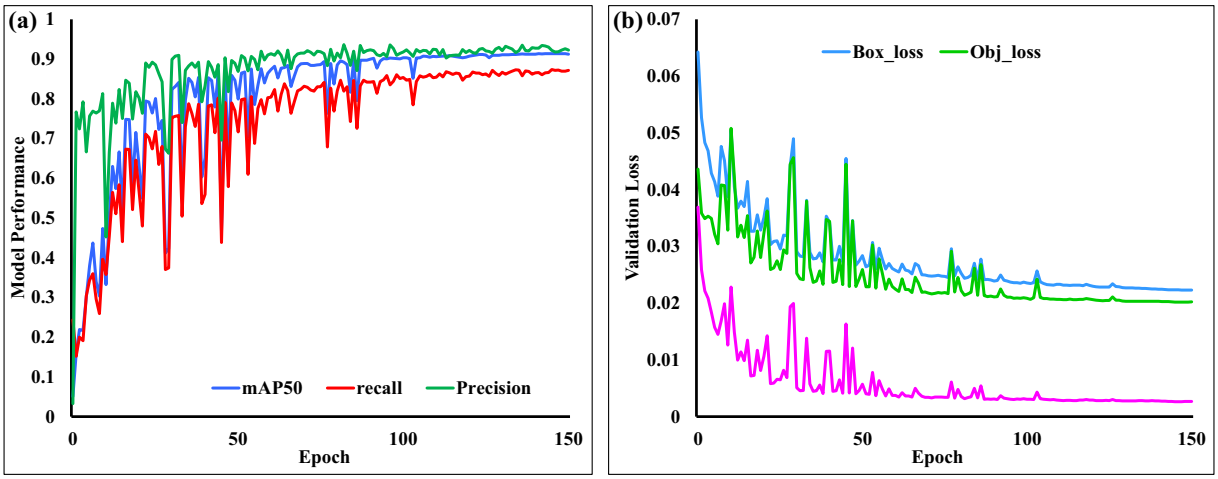

Fig. 6. (a) Progress of the testing performance of the models with the number of epochs. Precision, recall and mAP were used as the evaluation matrices, and (b) validation loss of models with the number of epochs.

thereby bringing down the number of sea turtle laying attempts (Lavers and Bond, 2017). This will lead to lowering the diversity of shoreline invertebrate communities and increasing the hazard of entanglement of coastal-nesting seabirds (Grant et al., 2021). The rate of accumulation of ML deposits around the RRI is high, especially on the windward side of the beaches. During the survey, we found many dead seabirds, especially Socotra cormorant (*Phalacrocorax nigrogularis*) along the windward beaches. *Phalacrocorax nigrogularis* is one of the least studied, regional endemic seabirds restricted to the Gulf and Oman coastal regions, and threatened by the anthropogenic disturbances (Muzaffar et al., 2017). In the marine environment, the seabirds are apex predators and well-known ecosystem engineers, capable of changing their terrestrial habitats by introducing marine-derived nutrients via deposition of guano and other allochthonous inputs. Therefore, when plastic accumulation increases in such remote uninhabited islands, even the pristine environments will become 'plastic islands' in long-run (Grant et al., 2021). Therefore, this cost effective machine learning (YOLO-v5) monitoring approach along with conventional methods can be implemented to other islands in the Gulf as well to estimate the ML load in the ROPME Sea region. This study could be an eye-opener to long-term monitoring program of ML across the ROPME Sea area to conserve marine ecosystem.

4. Conclusions

Worldwide, the remote islands receive unprecedented amount of ML, especially plastic waste. The implementation of machine learning YOLO-v5 algorithm in ML monitoring is relatively new in the Gulf region. This study provides a snapshot of spatial distribution, composition, sources and the possible biological impacts of ML around the Ras Rakan Island. Average ML abundance around the RRI is 3.4 items/m^2. The spatial distribution of ML exhibits higher densities in the windward beaches than the leeward beaches. Overall, 71% of items were derived from land-based sources, especially from neighbouring countries. Nearly 61% of sampling locations are found to be extremely dirty with higher amount of hazardous ML items. The prevailing winds, currents and Stokes drift in the Gulf play a major role in the transportation and deposition of ML on the RRI, and it is clear that RRI acts as a potential sink to ML deposition. In this study, the machine learning algorithm YOLO-v5 based model was applied for the detection, classification and quantification of ML in an uninhabited Island of Qatar. YOLO-v5 model has classified ML items with the precision of 0.91 (91%) mAP. The machine learning model results showed a significant positive relationship with the ML data obtained using a conventional method. Among the ML items, this machine learning model showed higher accuracy results for the plastic litter items than the other ML items. Machine learning results demonstrate that YOLO-v5 could complement conventional methods for the future ML monitoring programs. Therefore, it is recommended that the long-term integrated ML monitoring programs should be initiated in the Gulf using a combination of unmanned aerial vehicles, conventional methods and machine learning techniques with the involvement of government, private and public agencies for the effective conservation of marine ecosystem.

CRediT authorship contribution statement

S. Veerasingam: Conceptualization, Investigation, Methodology, Writing – original draft, Writing – review & editing. **Mark Chatting:** Investigation, Methodology, Writing – review & editing. **Fahad Syed Asim:** Investigation, Methodology, Writing – review & editing. **Jassim Al-Khayat:** Investigation, Methodology, Writing – review & editing. **P. Vethamony:** Writing – review & editing, Funding acquisition.

Declaration of Competing Interest

The authors declare that they have no known competing financial interests or personal relationships that could have appeared to influence the work reported in this paper.

Acknowledgements

We thank Prof. Hamad Al-Saad Al-Kuwari, Director, Environmental Science Center, Qatar University (QU) for his constant encouragement and support. We acknowledge ORS, QU for awarding the Project (QUEX-ESC-QP-TM-18/19) funded by the Qatar Energy. This work forms part of the award 'UNESCO Chair in Marine Sciences' related to the theme 'Marine pollution and Management'.

Appendix A. Supplementary data

Supplementary data to this article can be found online at https://doi.org/10.1016/j.scitotenv.2022.156064.

References

Al-Cibahy, A.S., Al-Khalifa, K., Boer, B., Samimi-Namin, K., 2012. Conservation of marine ecosystems with a special view to coral reefs in the Gulf. In: Riegl, B.M., Purkis, S.J. (Eds.), Coral Reefs of the Gulf: Adaptation to Climatic Extremes. Springer Science + Business Media B.V, pp. 740–755.

Alkalay, R., Pasternak, G., Zask, A., 2007. Clean-coast index – a new approach for beach cleanliness assessment. Ocean Coast. Manag. 50, 352–362.

Al-Khayat, J.A., Veerasingam, S., Aboobacker, V.M., Vethamony, P., 2021. Hitchhiking of encrusting organisms on floating marine debris along the west coast of Qatar, Arabian/Persian gulf. Sci. Total Environ. 776, 145985.
Al-Salem, S.M., Uddin, S., Al-Yamani, F., 2020. An assessment of microplastics threat to the marine environment: a short review in context of the Arabian/Persian gulf. Mar. Environ. Res. 159, 104961.
Andrades, R., Santos, R., Joyeux, J.-C., Chelazzi, D., Cincinelli, A., Giarrizzo, T., 2018. Marine debris in trindadeisland, a remote island of the South Atlantic. Mar. Pollut. Bull. 137, 180–184.
Arekhi, M., Terry, L.G., John, G.F., Al-Khayat, J.A., Castillo, A.B., Vethamony, P., 2020. Field and laboratory investigation of tarmat deposits found on RasRakan Island and northern beaches of Qatar. Sci. Total Environ. 735, 139516.
Barboza, L.G.A., Cozar, A., Gimenez, B.C.G., Barros, T.L., Kershaw, P.J., Guilhermino, L., Sheppard, C., 2019. Macroplastics Pollution in the Marine Environment. World Seas: An Environmental Evaluation, 2ndedn Academic Press, Cambridge, M.A, pp. 305–328.
Beaumont, N.J., Aanesen, M., Austen, M.C., Borger, T., Clark, J.R., Cole, M., Hooper, T., Lindeque, P.K., Pascoe, C., Wyles, K.J., 2019. Global ecological, social and economic impacts of marine plastic. Mar. Pollut. Bull. 142, 189–195.
Borrelle, S.B., Ringma, J., Law, K.L., Monnahan, C.C., Lebreton, L., McGivern, A., Murphy, E., Jambeck, J., Leonard, G.H., Hilleary, M.A., Eriksen, M., Possingham, H.P., Frond, H.D., Gerber, L.R., Polidoro, B., Tahir, A., Bernard, M., Mallos, N., Barnes, M., Rochman, C.M., 2020. Predicted growth in plastic waste exceeds efforts to mitigate plastic pollution. Science 369, 1515–1518.
Bosch, D.T., Dance, S.P., Moolenbeek, F.G., Oliver, P.G., 1995. Seashells of Eastern Arabia. Motivate Publishing, London 296p.
Burt, A.J., Raguain, J., Sanchez, C., Brice, J., Fleischer-Dogley, F., Goldberg, R., Talma, S., Syposz, M., Mahony, J., Letori, J., Quanz, C., Ramkalawan, S., Francourt, C., Capricieuse, I., Antao, A., Belle, K., Zillhardt, T., Moumou, J., Roseline, M., Bonne, J., Marie, R., Constance, E., Suleman, J., Turnbull, L.A., 2020. The costs of removing the unsanctioned import of marine plastic litter to small island states. Sci. Rep. 10, 14458.
Ditria, E.M., Lopez-Marcano, S., Sievers, M., Jinks, E.L., Brown, C.J., Connolly, R.M., 2020. Automating the analysis of fish abundance using object detection: optimizing animal ecology with deep learning. Front. Mar. Sci. 429.
EC JRC, 2013. European Commission, Joint Research Center. MSFD Technical Subgroup on Marine Litter (TSG-ML). Guidance on Monitoring of Marine Litter in European Seas. Scientific and Technical Research Series. Publications office of the European Union, Luxembourg, p. 128.
Fallati, L., Polidori, A., Salvatore, C., Saponari, L., Savini, A., Galli, P., 2019. Anthropogenic marine debris assessment with unmanned aerial vehicle imagery and deep learning: a case study along the beaches of the Republic of Maldives. Sci. Total Environ. 693, 133581.
Filho, W.L., Havea, P.H., Balogun, A.-L., Boenecke, J., Maharaj, A.A., Haapio, M., Hemstock, S.L., 2019. Plastic debris on Pacific Islands: ecological and health implications. Sci. Total Environ. 670, 181–187.
Galgani, F., Hanke, G., Werner, S., Oosterbaan, L., Nilsson, P., Fleet, D., 2013. Monitoring guidance for marine litter in European Seas. JRC Scientific and Policy Reports, Report EUR 26113 EN, p. 120.
Garcia-Garin, O., Monleon-Getino, T., Lopez-Brosa, P., Borrell, A., Aguilar, A., Borja-Robalino, R., Cardona, L., Vighi, M., 2021. Automatic detection and quantification of floating marine macro-litter in aerial images: introducing a novel deep learning approach connected to a web application in R. Environ. Pollut. 273, 116490.
Gomez, A.S., Scandolo, L., Eisemann, E., 2022. A learning approach for river debris detection. Int. J. Appl. Earth Obs. Geoinf. 107, 102682.
Goncalves, G., Andriolo, U., Pinto, L., Bessa, F., 2020. Mapping marine litter using UAS on a beach-dune system: a multidisciplinary approach. Sci. Total Environ. 706, 135742.
Grant, M.L., Lavers, J.L., Hutton, I., Bond, A.L., 2021. Seabird breeding islands as sinks for marine plastic debris. Environ. Pollut. 276, 116734.
Gregory, M.R., 2009. Environmental implications of plastic debris in marine settings – entanglement, ingestion, smothering, hangers-on, hitch-hiking and alien invasions. Philos. Trans. R. Soc. Lond. Ser. B Biol. Sci. 364, 2013–2025.
Hidaka, M., Matsuoka, D., Sugiyama, D., Murakami, K., Kako, S., 2022. Pixel-level image classification for detecting beach litter using a deep learning approach. Mar. Pollut. Bull. 175, 113371.
Ibrahim, E.A.A., Osman, N.A.R., Eisa, O.A.M., 2020. Status of the beach litter in the UNESCO world heritage site of dungonab and Mukkawar Island marine national park in Sudan, Red Sea. Int. J. Ecol. https://doi.org/10.1155/2020/6904745.
Iwasaki, S., Isobe, A., Kako, S., Uchida, K., Tokai, T., 2017. Fate of microplastics and mesoplastics carried by surface currents and wind waves: a numerical model approach in the sea of Japan. Mar. Pollut. Bull. 121, 85–96.
Jones, D.A., 1986. A Field Guide to the Seashores of Kuwait and the Arabian Gulf Kuwait. University of Kuwait 192p.
Kardousha, M.M., Al-Muftah, A., Al-Khayat, J.A., 2016. Exploring Sheraoh Island at southeastern Qatar: first distributional records of some island and offshore biota with annotated checklist. J. Mar. Sci. Res. Dev. 6, 191. https://doi.org/10.4172/2155-9910.1000191.
Kor, K., Mehdinia, A., 2020. Neustonicmicroplastic pollution in the Persian Gulf. Mar. Pollut. Bull. 150, 110665.
Kylili, K., Kyriakides, I., Artusi, A., Hadjistassou, C., 2019. Identifying floating plastic marine debris using a deep learning approach. Environ. Sci. Pollut. Res. 26, 17091–17099.
Kylili, K., Artusi, A., Hadjistassou, C., 2021. A new paradigm for estimating the prevalence of plastic litter in the marine environment. Mar. Pollut. Bull. 173, 113127.
Lavers, J.L., Bond, A.L., 2017. Exceptional and rapid accumulation of anthropogenic debris on one of the world's most remote and pristine islands. Proc. Natl. Acad. Sci. U. S. A. 114, 6052–6055.
Lavers, J.L., Dicks, L., Finger, A., 2019. Significant plastic accumulation on the cocos (keeling) islands, Australia. Sci. Rep. 9, 7102.
Lin, F., Hou, T., Jin, Q., You, A., 2021. Improved YOLO based detection algorithm for floating debris in waterway. Entropy 23, 1111.
Lyons, B.P., Cowie, W.J., Maes, T., Le Quesne, W.J.F., 2020. Marine plastic litter in the ROPME Sea area: current knowledge and recommendations. Ecotoxicol. Environ. Saf. 187, 109839.
Marin, I., Mladenovic, S., Gotovac, S., Zaharija, G., 2021. Deep-feature-based approach to marine debris classification. Appl. Sci. 11, 5644.
Mark, C., Hamza, S., Al-Khayat, J., Smyth, D., Husrevoglu, S., Marshall, C.D., 2021. Feminization of hawksbill turtle hatchlings in the twenty-first century at an important regional nesting aggregation. Endanger. Species Res. 44, 149–158.
Martin, C., Parkes, S., Zhang, Q., Zhang, X., McCabe, M.F., Duarte, C.M., 2018. Use of unmanned aerial vehicles for efficient beach litter monitoring. Mar. Pollut. Bull. 131, 662–673.
Martin, C., Zhang, Q., Zhai, D., Zhang, X., Duarte, C.M., 2021. Enabling a large-scale assessment of litter along saudi arabian red sea shores by combining drones and machine learning. Environ. Pollut. 277, 116730.
Maximenko, N., Hafner, J., Niiler, P., 2012. Pathways of marine debris derived from trajectories of lagrangian drifters. Mar. Pollut. Bull. 65, 51–62.
McIlgorm, A., Campbell, H.F., Rule, M.J., 2011. The economic cost and control of marine debris damage in the Asia-Pacific region. Ocean Coast. Manag. 54, 643–651.
MME, 2018. Ministry of Municipality and Environment. Removing 90 tons of wastes from RasRukn Island. http://www.mme.gov.qa/cui/view.dox?id=702&contentID=5449&siteID=2.
Monteiro, R.C.P., Ivar do Sul, J.A., Costa, M.F., 2018. Plastic pollution in islands of the Atlantic Ocean. Environ. Pollut. 238, 103–110.
Mugilarasan, M., Karthik, R., Purvaja, R., Robin, R.S., Subbareddy, B., Hariharan, G., Rohan, S., Jinoj, T.P.S., Anandavelu, I., Pugalenthi, P., Ramesh, R., 2021. Spatiotemporal variations in anthropogenic marine litter pollution along the northeast beaches of India. Environ. Pollut. 280, 116954.
Muzaffar, S.B., 2020. Socotra cormorants in the Arabian gulf: a review of breeding biology, feeding ecology, movements and conservation. Aquat. Ecosyst. Health Manag. 23 (2), 220–228.
Muzaffar, S.B., Whelan, R., Clarke, C., Gubiani, R., Benjamin, S., 2017. Breeding population biology in Socotra cormorants (Phalacrocoraxnigrogularis) in the United Arab Emirates. Waterbirds 40, 1–10.
Oliver, P.G., 1992. The Bivalve Seashells of the Red Sea. An Identification Guide. Christa Hemmenerlag, Wiesbaden and The National Museum of Wales, Cardiff 330p.
OSPAR, 2010. Guideline for Monitoring Marine Litter on the Beaches in the OSPAR Maritime Area. Edition 1.0. OSPAR Commission, London, UK 15pp.
Politikos, D.V., Fakiris, E., Davvetas, A., Klampanos, I.A., Papatheodorou, G., 2021. Automatic detection of seafloor marine litter using towed camera images and deep learning. Mar. Pollut. Bull. 164, 111974.
Rajendran, S., Al-Khayat, J.A., Veerasingam, S., Nasir, S., Vethamony, P., Sadooni, F.N., Al-Kuwari, H.A., 2021. WorldView-3 mapping of tarmat deposits of the RasRakan Island, northern coast of Qatar: environmental perspective. Mar. Pollut. Bull. 163, 111988.
Rangel-Buitrago, N., Adriana, G.C., Velez-Mendoza, A., Carvajal-Florian, A., Mojica-Martinez, L., Neal, W.J., 2019b. Where did this refuse come from? Marine anthropogenic litter on a remote island of the colombian Caribbean Sea. Mar. Pollut. Bull. 149, 110611.
Rangel-Buitrago, N., Vergara-Cortes, H., Barria-Herrera, J., Contreras-Lopez, M., Agredano, R., 2019a. Marine debris occurrence along las Salinas beach, VinaDel mar (Chile): magnitudes, impacts and management. Ocean Coast. Manag. 178, 104842.
Ranjani, M., Veerasingam, S., Venkatachalapathy, R., Jinoj, T.P.S., Guganathan, L., Mugilarasan, M., Vethamony, P., 2022. Seasonal variation, polymer hazard risk and controlling factors of microplastics in beach sediments along the southeast coast of India. Environ. Pollut. 305, 119315.
Redmon, J., Divvala, S., Girshick, R., Farhadi, A., 2016. You only look once: Unified, real-time object detection. Proceedings of the 2016 IEEE Conference on Computer Vision and Pattern Recognition, pp. 779–788.
Richmond, M.D., 2002. A Field Guide to the Seashores of Eastern Africa and the Western Indian Ocean Islands. Sida/Department of Research Cooperation, SAREC, and University of Dar es Salaam 461pp.
Sarafraz, J., Rajabizadeh, M., Kamrani, E., 2016. The preliminary assessment of abundance and composition of marine beach debris in the northern Persian Gulf, Bandar Abbas city, Iran. J. Mar. Biol. Assoc. U. K. 96, 131–135.
Savoca, M.S., McInturf, A.G., Hazen, E.L., 2021. Plastic ingestion by marine fish is widespread and increasing. Glob. Chang. Biol. https://doi.org/10.1111/gcb.15533.
Shabani, F.S., Nasrolahi, A., Thiel, M., 2019. Assemblage of encrusting organisms on floating anthropogenic debris along the northern coast of the Persian Gulf. Environ. Pollut. 254, 112979.
Shahdadi, A., Sari, A., Naderloo, R., 2014. A checklist of the barnacles (Crustacea: cirripedia: Thoracica) of the Persian Gulf and Gulf of Oman with nine new records. Zootaxa 3784, 201–223.
Teuten, E.L., Saquing, J.M., Knappe, D.R.U., Barlaz, M.A., Jonsson, S., Bjorn, A., Rowland, S.J., Thompson, R.C., Galloway, T.S., Yamashita, R., Ochi, D., Watanuki, Y., Moore, C., Viet, P.H., Tana, T.S., Prudente, M., Boonyatumanond, R., Zakaria, M.P., Akkhavong, K., Ogata, Y., Hirai, H., Iwasa, S., Mizukawa, K., Hagino, Y., Imamura, A., Saha, M., Takada, H., 2009. Transport and release of chemicals from plastics to the environment and to wildlife. Philos. Trans. R. Soc., B 364, 2027–2045.
Thiel, M., Luna-Jorquera, G., Alvarez-Varas, R., Gallardo, C., Hinojosa, I.A., Luna, N., Miranda-Urbina, D., Morales, N., Ory, N., Pacheco, A.S., Portflitt-Toro, M., Zavalaga, C., 2018. Impact of marine plastic pollution from continental coasts to subtropical gyres – fish, seabirds, and other vertebrates in the SE Pacific. Front. Mar. Sci. https://doi.org/10.3389/fmars.2018.00238.
Uddin, S., Fowler, S.W., Saeed, T., 2020. Microplastic particles in the Persian/Arabian gulf – a review on sampling and identification. Mar. Pollut. Bull. 154, 111100.

Veerasingam, S., Al-Khayat, J.A., Aboobacker, V.M., Hamza, S., Vethamony, P., 2020b. Sources, spatial distribution and characteristics of marine litter along the west coast of Qatar. Mar. Pollut. Bull. 159, 111478.

Veerasingam, S., Al-Khayat, J.A., Haseeba, K.P., Aboobacker, V.M., Hamza, S., Vethamony, P., 2020a. Spatial distribution, structural characterisation and weathering of tarmats along the west coast of Qatar. Mar. Pollut. Bull. 159, 111486.

Veerasingam, S., Vethamony, P., Aboobacker, V.M., Giraldes, A.M., Dib, S., Al-Khayat, J.A., 2021. Factors influencing the vertical distribution of microplastics in the beach sediments around the RasRakan Island, Qatar. Environ. Sci. Pollut. Res. 28, 34259–34268. https://doi.org/10.1007/s11356-020-12100-4.

Wang, K., Fang, B., Qian, J., Yang, S., Zhou, X., Zhou, J., 2019. Perspective transformation data agumentation for object detection. IEEE Access 8, 4935–4943.

Wu, W., Liu, H., Li, L., Long, Y., Wang, X., Wang, Z., Li, J., Chang, Y., 2021. Application of local fully convolutional neural network combined with YOLO v5 algorithm in small target detection of remote sensing image. PLoS ONE 16, e0259283.

Xia, C., Fu, L., Liu, H., Chen, L., 2018. In situ sea cucumber detection based on deep learning approach. Proceedings of the 2018 OCEANS-MTS/IEEE Kobe Techno-Oceans (OTO). IEEE, Piscataway, NJ, pp. 1–4.

Xu, W., Matzner, S., 2018. Underwater fish detection using deep learning for water power applications. Avialble at:arXiv [Preprint]. https://arxiv.org/abs/1811.01494.

Xu, R., Lin, H., Lu, K., Cao, L., Liu, Y., 2021. A forest detection system based on ensemble learning. Forests 12, 217.

Yu, S., Ma, J., 2021. Deep learning for geophysics: current and future trends. Rev. Geophys. 59, e2021RG000742.